Morphometric analysis of post-caldera monogenetic landforms at Deception Island, Antarctica: implications for hazard assessment

Dario Pedrazzi (1)*, Gabor Kereszturi (2), Augustin Lobo (1), Adelina Geyer (1), Janina Calle (3)

(1) ICTJA, CSIC, Group of Volcanology, SIMGEO UB-CSIC, Institute of Earth Sciences Jaume Almera, Lluis Sole i Sabaris s/n, 08028 Barcelona, Spain (*dpedrazzi@ictja.csic.es)
(2) Institute of Agriculture and Environment, Massey University, Palmerston North, New Zealand
(3) Gli Studies & Projects GLISP S.A., Principal Florida Norte s/n, Guayas, Guayaquil, Ecuador

EGU2019-1819

POSVOLDEC (CTM2016-79617-P)
(AEI/FEDER-UE)

1. INTRODUCTION

- Deception Island (DI), South Shetland Archipelago, Antarctica, is an excellent natural laboratory to study monogenetic volcanism as the post-caldera features are recent and well preserved.

- Post-caldera volcanism includes over 30 eruptions during the Holocene, although a considerably higher number of eruptions has been reported (e.g. *Orheim, 1971*).

- Recent eruptions in 1967, 1969 and 1970 (*Baker et al., 1975*; *Smellie, 2002*; *Pedrazzi et al., 2014; 2018*) have shown that volcanic activity on DI can become a concern for tourists, scientists and military personnel working on or near the island and it is not possible to rule out the possibility of a future eruption.

Southern view of Deception Island caldera. Picture taken from Telefon Bay. Credits Dario Pedrazzi (2013).

- One of the main problems is related to the lack of data about the ages of most of the edifices, in order to evaluate the eruptive recurrence.

- The objective of this work is to use the morphometric parameters of the craters and post-caldera volcanic edifices recognizable on the island, in order to assign them a relative age and complete the eruptive record of the island, as well as to determine morphometric differences between craters and volcanic edices product of different eruptive styles.

- This methodology has been used since the 70's to analyse mafic monogenetic volcanoes but it has not been fully developed until recently.

- Several works were carried out in Campo de Calatrava-Ciudad Real, Tenerife, Gran Canaria and Lanzarote (Spain), Mauna Kea (USA) and Highlands of Bakony-Balaton (Hungary).

2. GEOLOGICAL SETTING AND GENERAL CHARACTERISTICS OF DECEPTION ISLAND

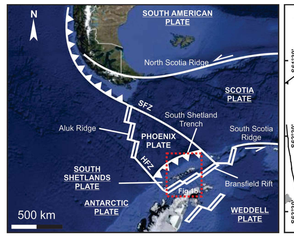

Simplified regional tectonic map and location of the South Shetland Islands Archipelago (modified from Ibañez et al., 2003). HFZ-Hero Fracture Zone, SFZ-Shetland Fracture Zone.

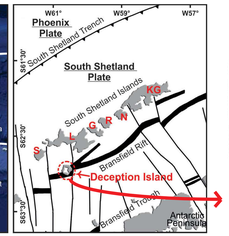

S-Snow Island, L-Livingston Island, G- Greenwich Island, R-Robert Island, N-Nelson Island, KG-King George Island.

- DI is located at the south-western end of the Bransfield Strait.

- DI consists of a horseshoe-shaped volcanic edifice (< 0.75 Ma; *Valencio et al., 1979*; Smellie, 1988).

- Three main phases lead to the formation of DI: pre-, syn- and post-caldera (*Smellie et al., 2002*; *Martí et al., 2013*).

- Historical post-caldera volcanism (1829–1970) on DI is characterised by monogenetic small-volume basaltic eruptions (< 0.1 km^3) of VEI 2 or 3 magnitude events.

- Recent explosive eruptions were driven by magma-water interaction, as the last eruptive episodes that took place between 1967 and 1970 (*Baker et al., 1975*; *Roobol, 1982*; *Smellie, 2001*; *Pedrazzi et al., 2014; 2018*).

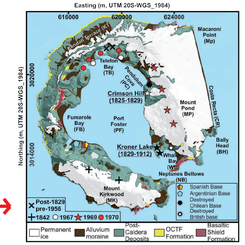

Simplified geological map of Deception Island (after Smellie et al., 2002; Martí et al., 2013).

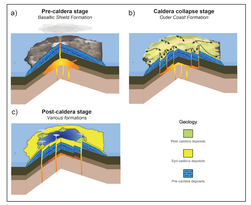

Simplified sketch illustrating the formation of the Deception Island caldera (after Martí et al., 2013).

3. METHODS

- Antarctic campaigns: RECALDEC in 2010-2011, PEVOLDEC in 2012-2013 and POSVOLDEC in 2017-2018;

- The source data used for the spatial localization, morphology and morphometric analysis of DI cones are:
i. the modified geological map of *Martí et al. (2013)*;
ii. the geomorphological map of the island at 1:25.000 (*López-Martínez et al., 2002*)
iii. the Digital Elevation Model (DEM), accuracy in a 2m x 2m raster.

- The morphometric parameters used in this study are:
i. Number of craters (Ncr);
ii. Crater maximum (Crmax) and minor (Crmin) diameter (i.e. *Wood, 1980a*);
iii. Cone height (Hcomax and Hcomin) (i.e. *Wood, 1980a*);
iv. Crater depth (Dcr) (i.e. *Carn, 2000*)
v. Cone major (Comax) and minor (Comin) diameter (i.e. *Wood, 1980a*).

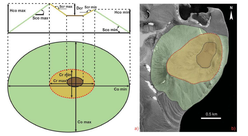

Morphometric parameters of DI's craters and cones.

- DEM-based slope angle calculations were performed to obtain Cone slope (Scomax and Scomin) and Crater slope (Scrmax and Scrmin) through the Quantum GIS, version Bonn (https://www.qgis.org/en/site/) and R-Studio software (https://www.rstudio.com/).

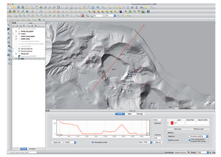

Quantum GIS, version Bonn.

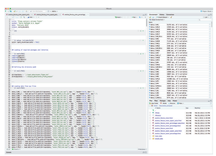

RStudio.

4. RESULTS

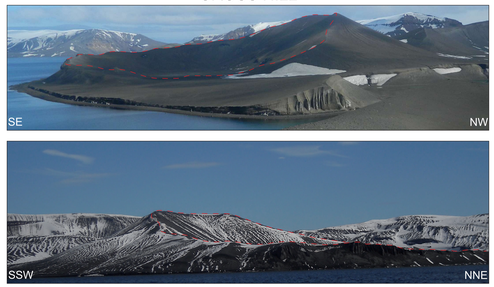

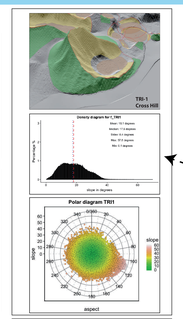

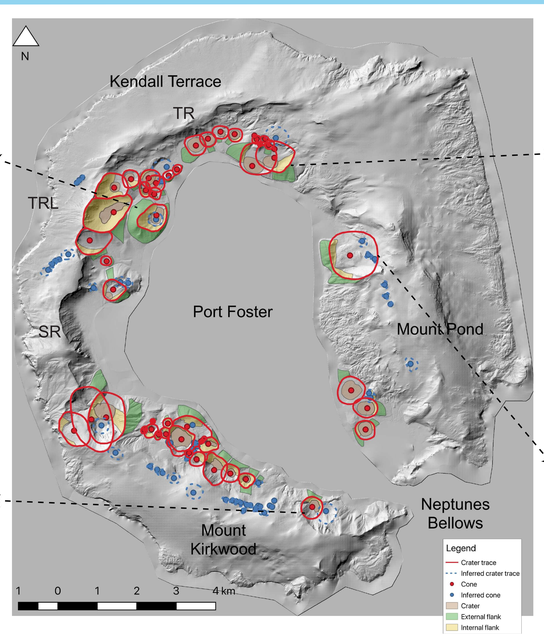

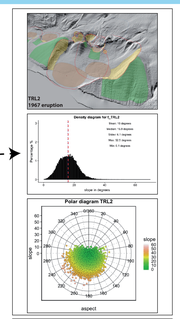

1967 ERUPTION LAND

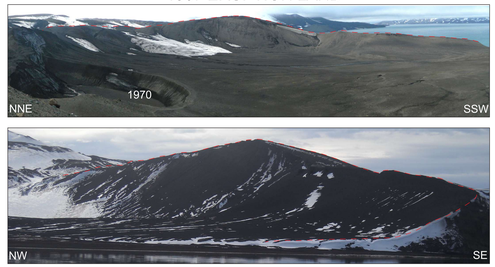

CRIMSON HILL

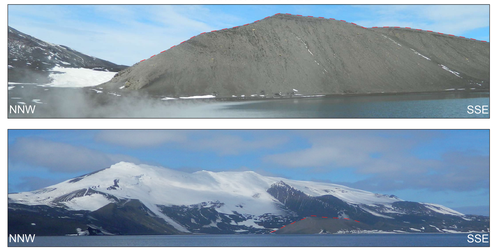

Map of DI cones and craters. 4 examples from different areas of the island are shown as well, including field pictures, 3D view from a DEM, density and polar diagrams.

5. DISCUSSION AND CONCLUSIONS

- At DI, more than 100 volcanic structures (including volcanic cones and/or craters) have been observed.

- In general, DI is a quite complex area in terms of morphometry; craters and cones show different morphologies and sizes.

- The island was divided into 5 zones:
i. Mount Kirkwood (MK) and Mount Pond (MP) correspond to the flanks with the highest topography;
ii. Telefon Ridge (Land Center) (TRL) and Telefon Ridge (Island Center) (TRI) correspond to the area with the least topography with centers in water;
iii. Stonethrow Ridge (SR) zone corresponds to the remaining section.

- Overlapping craters have been developed almost throughout the island being mostly in areas of greater topography.

- The histograms of slope angles of the volcanic structures at DI are complex since they present a multimodal and skewed distribution.

- If the volcanic structures were perfect, the frequency distribution of the slope histogram would be modal or symmetric, that is, the values of the mean, the median and the mode will coincide with each other.

- In the same way, polar diagrams show variabilities among the different volcanic landforms.

- This result can be associated with the mountainous relief that the area presents, where the volcanic structures have been seen, mostly, altered by erosive processes or by superposition of post - eruptive events, altering the morphology and causing the collapse of its volcanic structures. It is fundamental to consider magma-water interaction as well.

- Most of the volcanic structures identified for the analysis are located in the area of Mount Kirkwood whereas, on the contrary, it occurs with the area of Stonethrow Ridge. In this area there are less recognizable structures due to the degree of erosion and post-eruptive events (lava flows) that have altered the area or it could possibly be that there was less volcanic activity in recent times.

- At DI most of the monogenetic landforms are tuff cones (i.e. edifices as consequence of magma-water interaction) instead of scoria cones (only due to pure magmatic activity) as thought before.

- Preliminary results seem to show a general patter relating morphology and ages on the island although some more processing has to be done in order to get more reliable data.

- This information is important to reconstruct of the geological history of this volcanic area and to improve the volcanic hazard assessment at DI.

REFERENCES

-**Baker P.E., McReath I., Harvey M.R., Roobol M.J., Davies T.G. (1975).** The geology of the South Shetland Islands. V. Volcanic evolution of Deception Island. British Antarctic Survey. 78:81 PP.
-**Carn S. (2000).** The Lamongan volcanic field, East Java, Indonesia: physical volcanology, historic activity and hazards. J. Volcanol. Geotherm. Res. 95: 81–108.
-**Ibáñez J.M., Almendros J., Carmona E., Martí C., Abril, M. (2003).** The recent seismo-volcanic activity at Deception Island volcano. Deep-Sea Res II Top Stud Oceanogr 50(10):1611–1629.
-**López-Martínez J., Serrano, E. (2002).** Geomorphology. In: López-Martínez, J., Smellie,J.L., Thomson, J.W. & Thomson, M.R.A. (eds) Geology and Geomorphology of Deception Island. British Antarctic Survey, Cambridge, BAS GEOMAP Series, Sheets 6-A and 6-B, 1:25 000, 31-39.
-**Martí ,J, Geyer A., Aguirre-Díaz G. (2013).** Origin and evolution of the Deception Island caldera (South Shetland Islands, Antarctica). Bull Volcanol 75(6):732.
-**Orheim O. (1971).** Volcanic activity on Deception Island, South Shetland Islands. In: ADIE RJ (ed) Antarctic geology and geophysics. Universitetsforlaget, Oslo, pp 117–120.
-**Pedrazzi D., Aguirre-Díaz G., Bartolini S., Martí J., Geyer A. (2014).** The 1970 eruption on Deception Island (Antarctica): eruptive dynamics and implications for volcanic hazards. J Geol Soc 171(6):765–778.
-**Pedrazzi D., Németh K., Geyer A., Álvarez-Valero A. M., Aguirre-Díaz G., Bartolini, S. (2018).** Historic hydrovolcanism at Deception Island (Antarctica): implications for eruption hazards. Bulletin of Volcanology 80(1): 11.
-**Roobol M.J. (1982).** The volcanic hazard at Deception Island, South Shetland Islands. Brit Antarc Surv Bull 51:237-245.
-**Smellie JL (1988).** Recent observations on the volcanic history of Deception Island, South Shetland Islands. Brit Antarct Surv Bull 81:83
-**Smellie J.L. (2001).** Lithostratigraphy and volcanic evolution of Deception Island, South Shetland Islands. Antarct Sci 73(2):788–209.
-**Smellie J.L. (2002).** The 1969 subglacial eruption on Deception Island (Antarctica): events and processes during an eruption beneath a thin glacier and implications for volcanic hazards. Geol Soc Lond, Spec Publ 202(1):59–79.
-**Smellie J.L., López-Martinez J., Headland R.K., Hernández-Cifuentes F., Maestro A., Millar I.L., Rey J., Serrano E., Somoza L., Thomson J.W. (2002).** Geology and geomorphology of Deception Island. (BAS Geomap Series, Sheets 6A and 6B) 77pp.
-**Valencio D.A., Mendia J., Vilas J.F. (1979).** Palaeomagnetism and KAr age of Mesozoic and Cenozoic igneous rocks from Antarctica. Earth Planet Sci Lett 45(1):61–68.
-**Wood C.A. (1980a).** Morphometric analysis of cinder cone degradation. J Volcanol Geotherm Res 8(2–4):137–160.

FOR MORE INFORMATION

POSVOLDEC | ABOUT ME | ICTJA-CSIC

This research was supported by the MICINN grant CTM2011-13578-E and was partially funded by the POSVOLDEC project (CTM2016-79617-P) (AEI/FEDER-UE). A.G. is grateful for her Ramón y Cajal contract (RYC-2012-11024). D.P. is grateful for his Beatriu de Pinós (2016 BP 00086) contract.